

Study of all-angle negative refraction of light in metal–dielectric–metal multilayered structures based on generalized formulas of reflection and refraction

Jiangwei Chen^{1,2} · Jun Liu² · Weidong Xu²

Received: 12 November 2016 / Accepted: 2 August 2017 / Published online: 19 August 2017
© Springer-Verlag GmbH Germany 2017

Abstract In this paper, refraction behaviors of light in both metal single-layered film and metal–dielectric–metal multilayered films are investigated based on the generalized formulas of reflection and refraction. The obtained results, especially, dependence of power refractive index on incident angles for a light beam traveling through a metal–dielectric–metal multilayered structure, are well consistent with the experimental observations. Our work may offer a new angle of view to understand the all-angle negative refraction of light in metal–dielectric–metal multilayered structures, and provide a convenient approach to optimize the devised design and address the issue on making the perfect lens.

1 Introduction

Negative refraction, as one of the most interesting issues associated with metamaterials, has currently attracted considerable interest [1–7]. It has been predicted early from the coupled-wave theory that nanoscale metal waveguide arrays can achieve all-angle negative refraction [5, 6]. Recently, all-angle negative refraction of transverse magnetic (TM) polarized light and positive refraction of transverse electric (TE) polarized light in metal–dielectric–metal (MDM) multilayered structures are observed experimentally [7]. The measured power refractive index for TM polarized light is

approximately -1 over a broad range of incident angles, which closely matches the values obtained from analysis and simulations [7]. The measured power refractive index for TM polarized light is approximately -1 over a broad range of incident angles, which closely matches the values obtained from analysis and simulations [7]. However, deviation of the measured power refractive index from the expected values exists clearly in the range of low incident angles, which has not been fully understood yet.

It is known that a light beam traveling through a multilayered structure can be taken as a result of multiple reflections and transmissions of light in the device. Thus, the study of refraction behaviors of light in multilayered structure based on the reflection and refraction theory may give another angle of view to understand the observations reported in Ref. [7]. However, it is known early that the usual Snell's law is no longer valid at the lossy interface [8]. Several types of generalized Snell and Fresnel laws have been proposed previously [8–15]. It seems still difficult to predict the direction of energy flow of the transmitted light at a lossy interface. For example, two sets of typical equations were developed to study the situations for the light entering from the dielectric medium to the metal [12] or vice versa [13]. Detailed calculations show wrongly that the light path or the pseudo-refractive index will not be reversible and continuous in all-angle conditions [3, 4].

Recently, a new set of the generalized formulas of reflection and refraction is developed [16, 17], which may provide reasonable explanations for several refraction phenomena observed, e.g., the negative refraction occurring at lossy LHM/air interface obey the usual Snell's law [1, 2, 17], whereas negative refraction may also be produced by heavily lossy wedge without negative refractive index [3, 4, 14, 17, 18], and so on.

✉ Jiangwei Chen
jwchen69@163.com

¹ College of Electronic Science and Engineering, Nanjing University of Posts & Telecommunications, Nanjing 210046, People's Republic of China

² National Key Laboratory of Electromagnetic Environmental Effects & Optoelectric Engineering, Nanjing 210007, People's Republic of China

In this work, we shall demonstrate our study of refraction behaviors of light in MDM multilayered structure based on the generalized formulas of reflection and refraction [16, 17], and show that the obtained results are well consistent with the observations reported in Ref. [7]. The remainder of the paper is organized as follows: in Sect. 2, the generalized formulas of reflection and refraction are introduced briefly. In Sect. 3, several properties of transmitted light associated with noble metal films are investigated numerically. Finally, some conclusions are drawn in Sect. 4.

2 Formulas and analysis

Let us begin by considering the case that a light beam is obliquely incident at a lossy interface. For simplicity, the media are assumed to be homogeneous isotropic and linear, which can be represented by the complex scalar relative permittivity $\tilde{\epsilon} = |\tilde{\epsilon}| \exp(j\alpha_\epsilon)$ and permeability $\tilde{\mu} = |\tilde{\mu}| \exp(j\alpha_\mu)$, respectively. Here $\alpha_{\epsilon(\mu)}$ is electric (magnetic) damping angle. (In this paper, time harmonic $e^{-j\omega t}$ is chosen, and the complex valued parameters are marked with superscript “~”). It is stressed that, when a beam of light propagates in a lossy medium, its electromagnetic parameters of $\tilde{E}(t)$, $\tilde{D}(t)$, $\tilde{H}(t)$ and $\tilde{B}(t)$ usually oscillate non-synchronously. To treat non-synchronized oscillation of $\tilde{H}(t)$, $\tilde{E}(t)$ and $\tilde{D}(t)$, the generalized formulas of reflection and refraction derived from the real valued time-dependent boundary conditions are, respectively, given as [16, 17]:

$$\theta_r^{TM} = \theta_i^{TM}, \tag{1a}$$

$$b_t^{TM} \sin \theta_t^{TM} = b_i^{TM} \sin \theta_i^{TM}, \tag{1b}$$

$$T_H^{TM} \equiv \frac{\text{Re}(\tilde{H}_t^{TM}(t))}{\text{Re}(\tilde{H}_i^{TM}(t))} = \frac{a_i^{TM} \cos \theta_i^{TM} + a_r^{TM} \cos \theta_r^{TM}}{a_r^{TM} \cos \theta_r^{TM} + a_t^{TM} \cos \theta_t^{TM}}, \tag{1c}$$

$$\Gamma_H^{TM} \equiv \frac{\text{Re}(\tilde{H}_r^{TM}(t))}{\text{Re}(\tilde{H}_i^{TM}(t))} = \frac{a_i^{TM} \cos \theta_i^{TM} - a_t^{TM} \cos \theta_t^{TM}}{a_r^{TM} \cos \theta_r^{TM} + a_t^{TM} \cos \theta_t^{TM}}, \tag{1d}$$

$$\theta_r^{TE} = \theta_i^{TE}, \tag{2a}$$

$$b_t^{TE} \sin \theta_t^{TE} = b_i^{TE} \sin \theta_i^{TE}, \tag{2b}$$

$$T_E^{TE} \equiv \frac{\text{Re}(\tilde{E}_t^{TE}(t))}{\text{Re}(\tilde{E}_i^{TE}(t))} = \frac{a_i^{TE} \cos \theta_i^{TE} + a_r^{TE} \cos \theta_r^{TE}}{a_r^{TE} \cos \theta_r^{TE} + a_t^{TE} \cos \theta_t^{TE}}, \tag{2c}$$

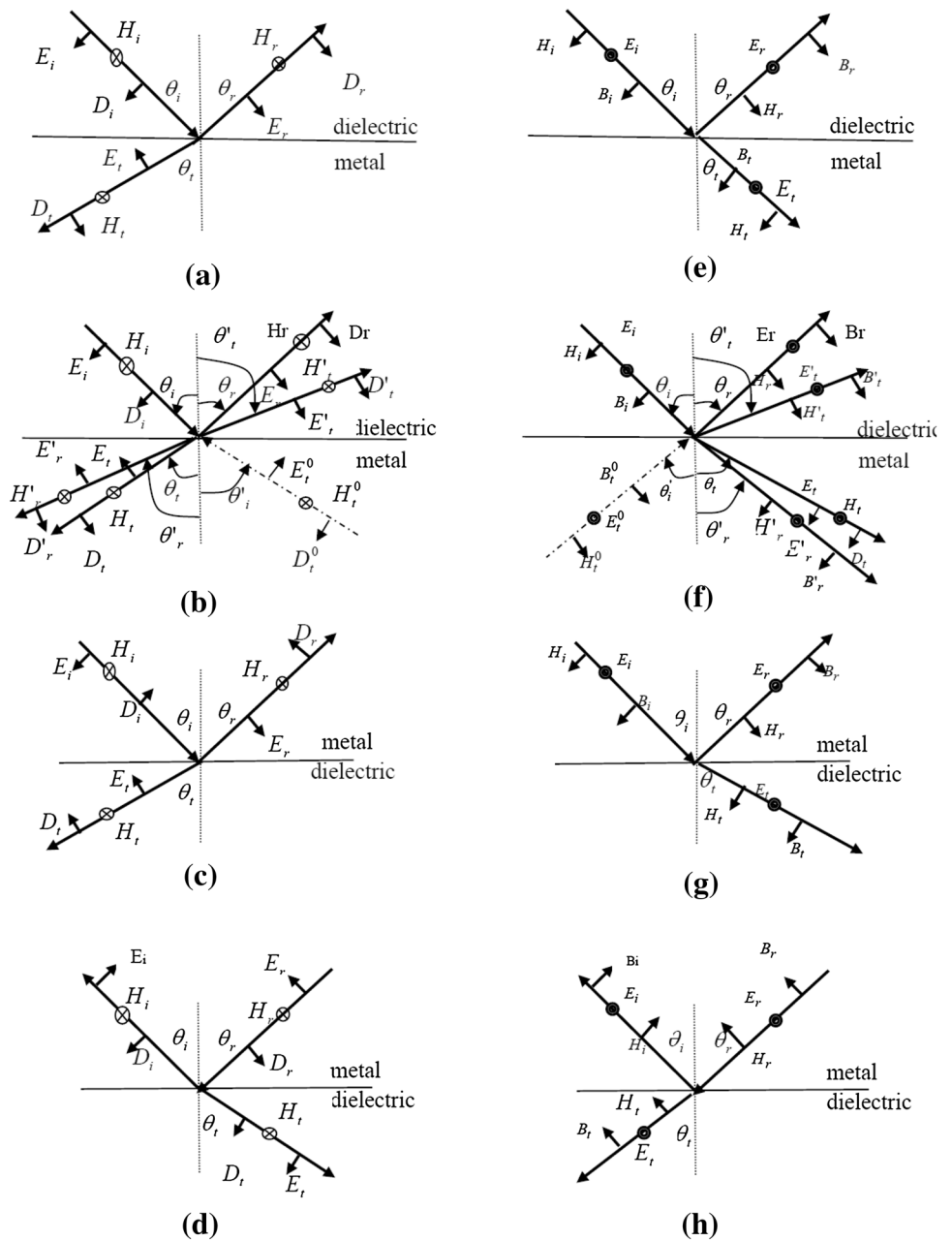
$$\Gamma_E^{TE} \equiv \frac{\text{Re}(\tilde{E}_r^{TE}(t))}{\text{Re}(\tilde{E}_i^{TE}(t))} = \frac{a_i^{TE} \cos \theta_i^{TE} - a_t^{TE} \cos \theta_t^{TE}}{a_r^{TE} \cos \theta_r^{TE} + a_t^{TE} \cos \theta_t^{TE}}, \tag{2d}$$

where, TE (TM) refers to the TE (TM) polarized light, all angles of θ_i^{TE} , θ_r^{TE} , θ_t^{TE} , θ_i^{TM} , θ_r^{TM} and θ_t^{TM} are real valued and relate to the true physical path of the incident, reflected and transmitted lights, respectively (see Fig. 1). $b_\zeta^{TM} = \text{Re}(\tilde{k}_\zeta) - \text{Im}(\tilde{k}_\zeta) \text{Im}(\tilde{H}_\zeta^{TM}(t)) / \text{Re}(\tilde{H}_\zeta^{TM}(t))$ [since $\text{Re}(\tilde{D}_\zeta^{TM}(t)) = \text{Re}(\tilde{k}_\zeta \tilde{H}_\zeta^{TM}(t)) \equiv b_\zeta^{TM} \text{Re}(\tilde{H}_\zeta^{TM}(t))$, $\tilde{k}_\zeta = \frac{\omega}{c} \sqrt{\tilde{\mu}_\zeta \tilde{\epsilon}_\zeta}$ is wave vector], $a_\zeta^{TM} = \text{Re}(\tilde{\eta}_\zeta) - \text{Im}(\tilde{\eta}_\zeta) \text{Im}(\tilde{H}_\zeta^{TM}(t)) / \text{Re}(\tilde{H}_\zeta^{TM}(t))$ [since $\text{Re}(\tilde{E}_\zeta^{TM}(t)) = \text{Re}(\tilde{\eta}_\zeta \tilde{H}_\zeta^{TM}(t)) \equiv a_\zeta^{TM} \text{Re}(\tilde{H}_\zeta^{TM}(t))$, $\tilde{\eta}_\zeta = \sqrt{\tilde{\mu}_\zeta \mu_0 / \tilde{\epsilon}_\zeta \epsilon_0}$ is wave impedance], $b_\zeta^{TE} = \text{Re}(\tilde{k}_\zeta) - \text{Im}(\tilde{k}_\zeta) \text{Im}(\tilde{E}_\zeta^{TE}(t)) / \text{Re}(\tilde{E}_\zeta^{TE}(t))$ [since $\text{Re}(\tilde{B}_\zeta^{TE}(t)) = \text{Re}(\tilde{k}_\zeta \tilde{E}_\zeta^{TE}(t)) \equiv b_\zeta^{TE} \text{Re}(\tilde{E}_\zeta^{TE}(t))$], $a_\zeta^{TE} = [\text{Re}(\tilde{\eta}_\zeta) + \text{Im}(\tilde{\eta}_\zeta) \text{Im}(\tilde{E}_\zeta^{TE}(t)) / \text{Re}(\tilde{E}_\zeta^{TE}(t))] / \tilde{\eta}_\zeta \tilde{\eta}_\zeta^*$ [since $\text{Re}(\tilde{H}_\zeta^{TE}(t)) = \text{Re}(\tilde{\eta}_\zeta^{-1} \tilde{E}_\zeta^{TE}(t)) \equiv a_\zeta^{TE} \text{Re}(\tilde{E}_\zeta^{TE}(t))$], $\zeta = i, r, t$ refer to the incident, reflected and transmitted light beams, and $\xi = 1, 2$ indicate the two media at the two sides of the interface, respectively.

Here, we shall focus on refraction behaviors of light at the interface formed by noble metal and lossless dielectric. Neglecting the small imaginary part of permittivity of the noble metal, the noble metal permittivity is approximately taken as a negative real number [19], which indicates that direction of $\tilde{D}(t)$ ($\equiv \text{Re}(\tilde{D}(t))$) in the noble metal is contrary to that of $\tilde{E}(t)$ ($\equiv \text{Re}(\tilde{E}(t))$). All possible direction relationships among electric and magnetic parameters of the incident, reflected and transmitted lights at both lossless dielectric-noble metal and noble metal-lossless dielectric interfaces are presented in Fig. 1 [17]. For TM polarized light, it is found from Fig. 1a–c that, to satisfy the real valued boundary conditions, the refracted angle is negative. Figure 1d refers to the case that time-dependent Poynting vector (TDPV) of the incidence propagates away from the interface, simultaneously, TDPV of reflected light propagates toward the interface. Thus the usual defined reflected light beam plays a role as an incidence [17]. On the other hand, it is seen from Fig. 1e–g that refraction of obliquely incident TE polarized light is positive. Figure 1h is similar to the case shown in Fig. 1d. Taking into account effects of imaginary parts of permittivity of both the dielectric and metal, the properties of the transmitted light may refer to Ref. [17], it is demonstrated that negative refraction of TM polarized light and positive refraction of TE polarized one may occur at the interface formed by lossless (low lossy) dielectric and nonmagnetic noble metal, which may be mainly attributed to the significant difference between α_ϵ and α_μ of the noble metal.

Based upon Eqs. (1), (2), we can further investigate properties of a light beam traveling through a single-layered or multi-layered film. As shown in Fig. 2, a beam of light traveling

Fig. 1 Sketch of possible direction relationships among electric and magnetic parameters of incident, reflected and refracted lights at the lossless dielectric–noble metal and noble metal–lossless dielectric interfaces (neglecting the imaginary part of ϵ_{metal}). **a–d** for TM polarized light (\otimes refer the magnetic field toward insider), **e–h** for TE polarized light (\bullet refer the electric field toward outsider), respectively. The real valued angles of θ_i , θ_r and indicate incident, reflected and refracted angles, respectively. Angles of θ'_i , θ'_r and θ'_t in **b** and **f** are the incident, reflected and refracted angles respecting to the case that the usual defined transmitted light plays a role as an incidence due to its TDPV propagating toward the interface



through a MDM multilayered structure is taken as a result of the light beam reflects and refracts at an interface and then propagates through a layer of homogeneous film step by step (For simplicity, the reflected light beams are neglected in Fig. 2). At an interface, the time dependent refracted angle $\theta_t^{\text{TM(TE)}}$, fields of $H_S^{\text{TM(TE)}}(t)$ and $E_S^{\text{TM(TE)}}(t)$ are calculated by using Eqs. (1), (2), propagation of light in the layer of homogeneous film is considered by the term of $e^{-\text{Im}(k) \cdot r}$ (r is the propagation distant of the light). Adopting the coordinate axis x given in Fig. 2, when the light travel through the final interface, the TDPV of transmitted light is given as:

$$\vec{S}_t^{\text{TM(TE)}}(x, t) \equiv \text{Re} \left(\vec{E}_t^{\text{TM(TE)}}(t) \right) \times \text{Re} \left(\vec{H}_t^{\text{TM(TE)}}(t) \right) \quad (3)$$

Further, the time-averaged Poynting vector (TAPV) of the transmitted light is obtained as:

$$\left\langle \vec{S}_t^{\text{TM(TE)}}(x) \right\rangle \equiv \sum_{t=0}^{T_{\text{period}}} \vec{S}_t^{\text{TM(TE)}}(x, t) \Delta t / T_{\text{period}} \quad (4)$$

3 Simulations and discussions

We firstly consider the cases that a beam of light travels through a silver single-layered film. The wavelength of the light in free-space is chosen as $\lambda = 363.8$ nm. It is noted that

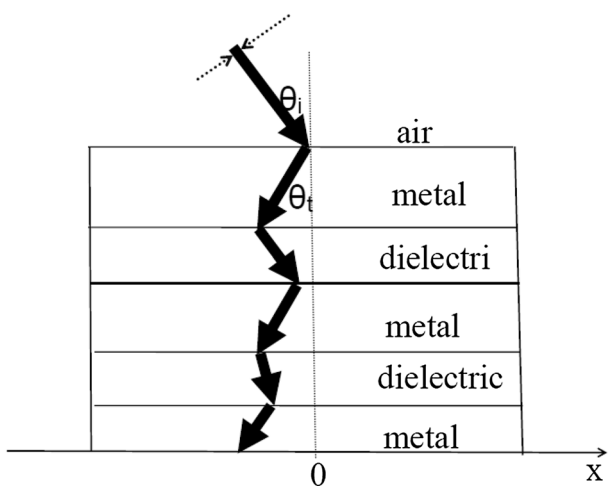


Fig. 2 Sketch of a light beam with certain width travels through a MDM multilayered structure. For simplicity, the reflected light beams are neglected

permittivity $\tilde{\epsilon}_{Ag}(\omega)$ of silver depends sensitively on the light frequency. In addition, the imaginary part $\text{Im}(\tilde{\epsilon}_{Ag}(\omega))$ may be strongly affected by several factors, such as surrounding media, the dimensions and shapes of the elements, etc. [19]. Here, according to Eq. (1) in Ref. [19], the silver permittivity is approximately taken as $\tilde{\epsilon}_{Ag} = -2.1 + j0.5$. Assuming the incident light beam to be very narrow and choosing the film thickness as $h = 20$ nm, TAPV of the transmission are calculated by using Eqs. (1)–(4) and shown in Fig. 3a. It is noted that TAPV of the transmission distributes in a certain range along the x axis, a peak of TAPV curve for TM polarized light locates in negative side of x axis, whereas, a peak of TAPV curve for TE polarized light locates in positive side of x axis. According to the peak position x_{peak} , the refracted angle is given as $\theta_{\text{peak}} = \arctan(x_{\text{peak}}/h)$. Furthermore, the power refractive index is defined as $n_s = \sin(\theta_i)/\sin(\theta_{\text{peak}})$ [7]. From the dependence of n_s on incident angles given in Fig. 3b, it is found that, although n_s value may alter slightly with change of the incident angle, n_s is always negative for

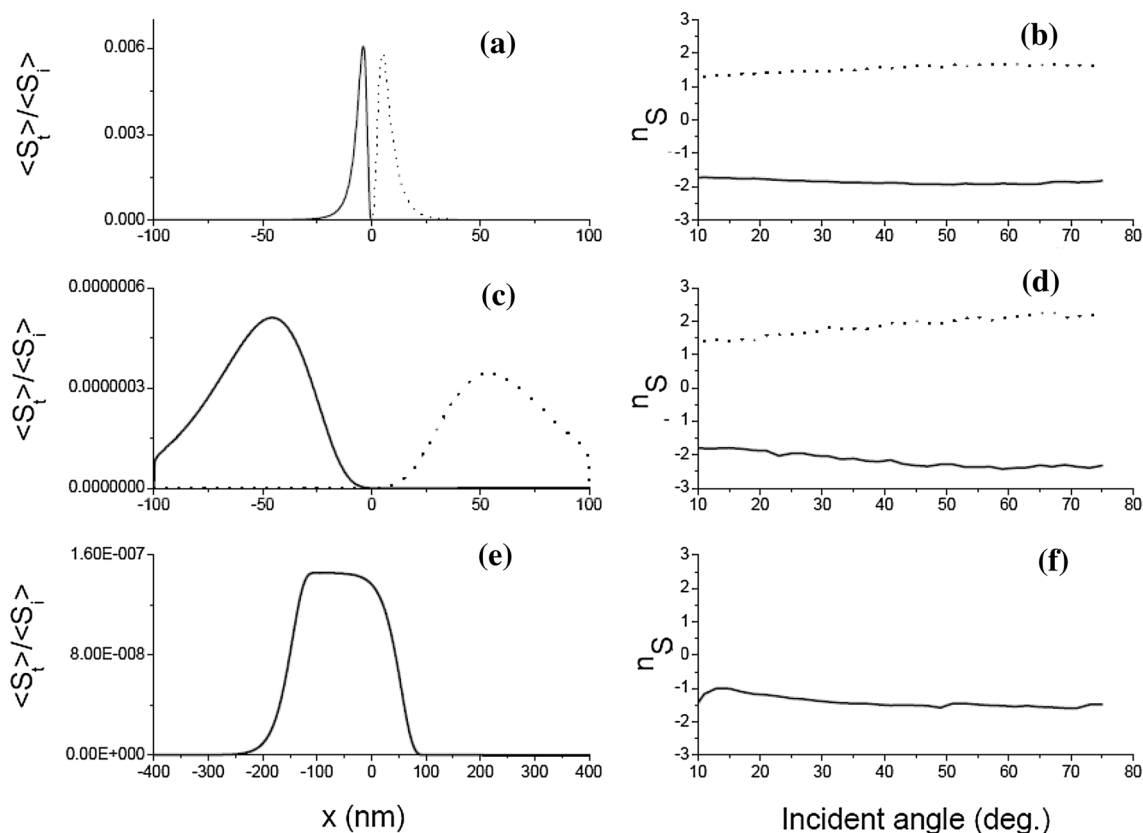


Fig. 3 Transmission of obliquely incident light beams ($\lambda = 363.8$ nm) through a silver single-layered film. Assuming that the incident light beam is very narrow and choosing film thickness as, **a** TAPV of the transmitted light $\langle |S_t|^2 \rangle$ ($\theta_i = 20^\circ$) and **b** power refractive index n_s versus incident angles, respectively. Increasing the film thickness to be 150 nm, **c** $\langle |S_t|^2 \rangle$ ($\theta_i = 20^\circ$)

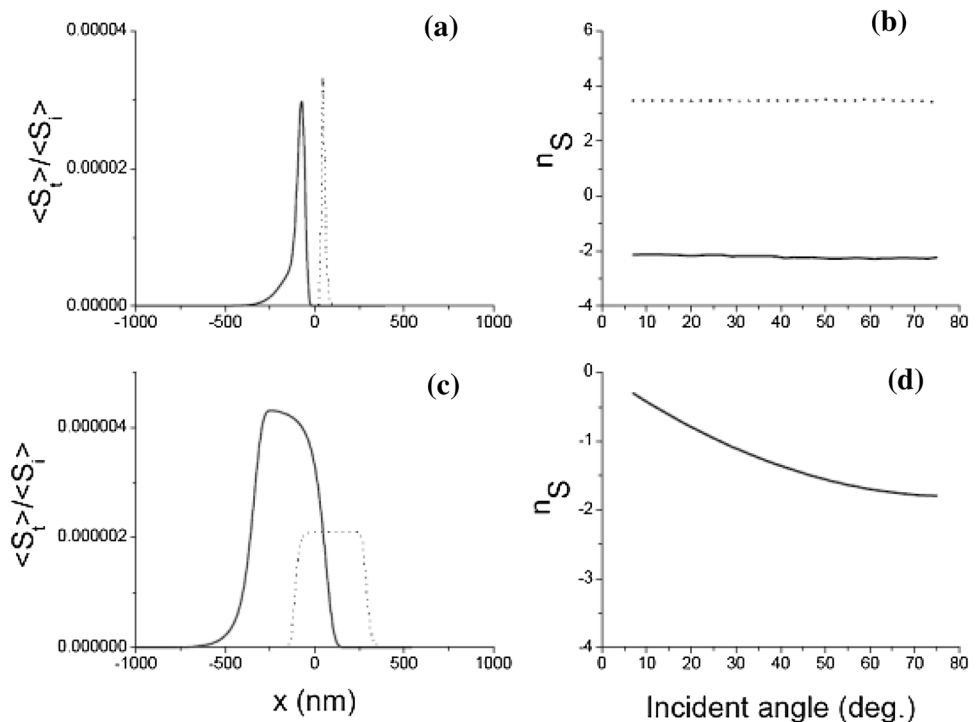
and **d** n_s , respectively. Taking width of the incident light beam as 400 nm and the film thickness as 150 nm, **e** $\langle |S_t|^2 \rangle$ ($\theta_i = 20^\circ$) and **f** n_s , respectively. The solid (dotted) lines refer to TM (TE) polarized light

TM polarized light and positive for TE polarized light, which indicates that all-angle negative refraction of TM polarized light may occur in a silver single-layered film. Increasing the film thickness to be $h = 150$ nm, it is seen from Fig. 3c that distribution range of TAPV along x axis extends. In addition, $|n_S|$ becomes larger than that of the thinner film when the incident angle is somewhat large (see Fig. 3d), which may be attributed to the energy losses in the film. On the other hand, it is noted from Fig. 3a, c that peak shapes of TAPV curves are asymmetric. We shall demonstrate that the asymmetric peak of TAPV curve may lead $|n_S|$ to depend on the width of the incident light beam (width of the incident light beam refers to Fig. 2). Choosing width of the incident light beam as 400 nm and the film thickness as $h = 150$ nm, the calculated results are shown in Fig. 3e, f, it is clear that both the peak shape of the TAPV curve and value of n_S are significantly different with the cases shown in Fig. 3a–d, respectively. Further increasing width of the incident light beam may flatten the top of TAPV curve peak. Taking x_{peak} as the center position of the flat top of TAPV curve peak, n_S is no longer altered by further increasing the width of the incident light beam. Additionally, we shall point out that value of $|n_S|$ increases with increasing either $|\text{Re}(\tilde{\epsilon}_{\text{Ag}}(\omega))|$ or $|\text{Im}(\tilde{\epsilon}_{\text{Ag}}(\omega))|$. Apparently, our simulations indicate that $|n_S|$ of a lossy film depends on several factors, which is strongly different from that of a lossless film.

Then we consider the cases that a beam of light ($\lambda = 363.8$ nm) travels through a MDM multilayered structure. The adopted structure is formed by three vertically

stacked MDMDM (metal, Ag; dielectric, TiO_2) unit cells as given in Fig. 1a in Ref. [7]. Analogously, the individual layer thicknesses of the MDMDM layers are taken as 33, 28, 30, 28 and 33 nm, respectively. We noted that permittivity $\tilde{\epsilon}_{\text{TiO}_2}(\omega)$ of TiO_2 is significantly dependent on the light frequency and film thickness. Here, the TiO_2 permittivity is approximately taken as $\tilde{\epsilon}_{\text{TiO}_2} = (4.3 + j0.2)^2 = 18.4 + j1.7$ [20]. Assuming the incident light beam to be very narrow, TAPV of the transmission and n_S are calculated and presented in Fig. 4a, b, respectively, which clearly demonstrate that refraction of TM polarized light is negative and refraction of TE polarized light is positive. Comparing Fig. 4a, b with Fig. 3a, b, it is found that the value of n_S is altered by the embedded TiO_2 layers, lead $|n_S|$ of TM polarized light to become apparently smaller than that of TE polarized light, thus $|x_{\text{peak}}|$ of TM polarized light is significantly larger than that of TE polarized light, which is consistent with the observations given in Fig. 2b in Ref. [7]. Taking the width of incident light beam as 400 nm, the calculated results are shown in Fig. 4c, d, respectively. It is clear that shape of TAPV peak of the TM polarized light is asymmetric, which is consistent with the third case given in Fig. 2b ($\theta_i = 40^\circ$) in Ref. [7], in addition, value of n_S and dependence of n_S on incident angles is good in agreement with the measured results presented in Fig. 2c in Ref. [7]. It is noted that, comparing with the numerical results obtained by using other methods and given Fig. 2c in Ref. [7], our calculated results shown in Fig. 4d are more close to the experimental observations. Therefore, the negative refraction of TM polarized light in

Fig. 4 Transmission of obliquely incident light beams ($\lambda = 363.8$ nm) through a MDM multilayered structure. Assuming that the incident light beam is very narrow, **a** $\langle S_t \rangle$ ($\theta_i = 20^\circ$) and **b** n_S , respectively. Choosing the incident light beam width as 400 nm, **c** $\langle S_t \rangle$ ($\theta_i = 40^\circ$), and **d** n_S , respectively. The *solid* (*dotted*) lines refer to TM (TE) polarized light



the MDM multilayered structure may be mainly attributed to the negative refraction of light at the noble metal-dielectric interfaces and effects of width of the incident light beam. We shall stress that TAPV curve of the transmitted light may be affected by other factors, such as the properties of the incident light and diffraction associated with the limit width of the aperture. Considering carefully effects of these factors may lead the calculated results to be further in agreement with the experimental observations.

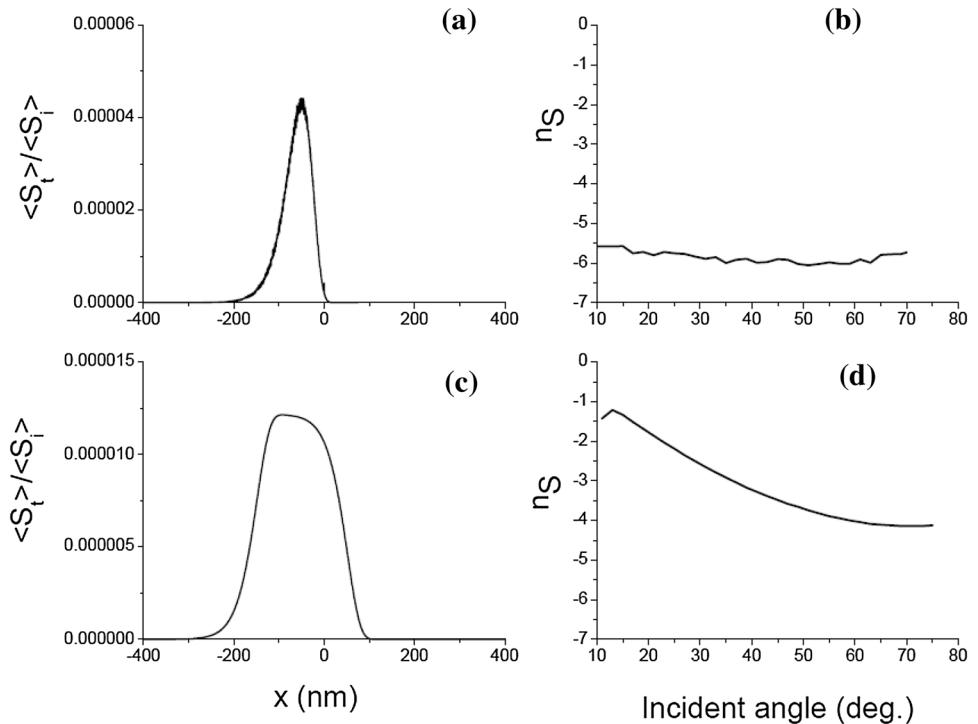
Thirdly, we shall simply address effects of the symmetry of the waveguide modes, which is demonstrated to be crucial to the realization of negative refraction in the metamaterial [6]. However, according to our model (see Fig. 2) and calculated results, the symmetry of the waveguide modes is not necessary. If so, design and preparation of MDM multilayered structure with negative n_s may be simplified.

Fourthly, we shall discuss dependence of n_s on light wavelength. As an instance, choosing wavelength of the light in free-space as $\lambda = 400$ nm, thus permittivities of Ag and TiO_2 layers become approximately to be $\tilde{\epsilon}_{\text{Ag}} = -4.43 + j0.21$ and $\tilde{\epsilon}_{\text{TiO}_2} = 12.24$ [6], respectively. Adopting same MDM multilayered structure mentioned above, the calculated results presented in Fig. 5 clearly demonstrate that, here, power refractive index n_s for TM polarized light is approximately in the range from -1 to -4 , which differs to the n_s shown in Fig. 4 and indicates significant dependence of n_s on light wavelength. It is noted that refraction of light at the pure Au/air interface may go from negative to positive with increasing the frequency [4], which may be attributed to the

decrease of electric damping angle of the Au permittivity with increasing light frequency [17, 18]. Our study predicts that light refraction may go from negative to positive in the visible region if the Ag layers in the adopted MDM multilayered structure are replaced by the Au ones.

Finally, we shall pay some attention on several theoretical methods have been applied to study light refraction phenomena associated with lossy interface [9–15]. At an interface formed by lossless medium with refractive index of n_a and lossy medium with complex refractive index of $n + j\kappa$, the Snell's law may be modified as $n_m \sin \theta_m = n_a \sin \theta_a$, where the pseudo-refractive index n_m and the real angle θ_m at the lossy medium side are a function of n_a , $n + j\kappa$ and incident angle θ_i [3, 4, 12, 13]. When the light travel from lossless medium into lossy medium with incident angle of θ_i , there are [12] $\theta_a = \theta_i$, $n_m = \sqrt{n_a^2 \sin^2 \theta_a + q^2(n \cos \gamma - k \sin \gamma)^2}$, $q^2 \cos 2\gamma = 1 - n_a^2 \sin^2 \theta_a (n^2 - \kappa^2)/(n^2 + \kappa^2)^2$, $q^2 \sin 2\gamma = 2n\kappa n_a^2 \sin^2 \theta_a / (n^2 + \kappa^2)^2$. Whereas, for the case of light travel from lossy medium into lossless medium with incident angle of θ_i , there are [13] $\theta_m = \theta_i$, $n_m = n / \sqrt{n^2 \sin^2 \theta_m / n_a^2 + q^2 \cos^2 \gamma}$, $q^2 \cos 2\gamma = 1 - \sin^2 \theta_m (n^2 - \kappa^2) / n_a^2$, $q^2 \sin 2\gamma = -2n\kappa \sin^2 \theta_m / n_a^2$. It is noted that both n_a and n_m are always positive at the Ag/TiO₂ interface when permittivity of Ag and TiO₂ are approximately taken as $\tilde{\epsilon}_{\text{Ag}} = -2.1 + j0.5$ and $\tilde{\epsilon}_{\text{TiO}_2} = 18.4$, respectively. In addition, both TM and TE polarized lights obey the same modified Snell's law, thus neither negative refraction of TM polarized light nor different propagation direction between TE and TM

Fig. 5 Transmission of obliquely incident TM polarized light beams ($\lambda = 400$ nm) through a MDM multilayered structure. Assuming that the incident light beam is very narrow, **a** $\langle S_t \rangle$ ($\theta_i = 40^\circ$) and **b** n_s , respectively. Choosing width of the incident light beam as 400 nm, **c** $\langle S_t \rangle$ ($\theta_i = 40^\circ$) and **d** n_s , respectively



polarized transmitted lights can be obtained by using this modified Snell's law. On the other hand, according to the energy streamline method [15, 21], the negative refraction for TM polarized light and positive refraction for TE polarized light are predicted to occur at the interface formed by nonmagnetic noble metal and dielectric, n_S which is attributed to the negative real part of the noble metal permittivity. However, this prediction seems not valid for the positive refraction of light occurring at the Au/air interface [4, 21]. Therefore, the observed refraction phenomena associated with energy losses may provide a possibility to test and develop the generalized Snell and Fresnel laws.

4 Conclusions

In summary, based on the generalized formulas of reflection and refraction, we have demonstrated that negative refraction of TM polarized light and positive refraction of TE polarized light in the MDM multilayered structure are mainly attributed to refraction behaviors of light at the noble metal–dielectric interfaces. In addition, the value of n_S may be affected by several factors. Our work suggests a common basis for the negative refraction occurred at noble metal–air interface, in noble metal single-layered film and MDM multilayered structure, provides a convenient approach to optimize the devised design and address the issue on making the perfect lens.

References

1. R.A. Shelby, D.R. Smith, S. Schultz, Experimental verification of a negative index of refraction. *Science* **292**, 77–79 (2001)
2. C.G. Parazzoli, R.B. Gregor, K. Li, B.E.C. Koltenbah, M. Tanielian, Experimental verification and simulation of negative index of refraction using Snell's law. *Phys. Rev. Lett.* **90**, 107401 (2003)
3. Y.H. Wu, W. Gu, Y.R. Chen, Z.H. Dai, W.X. Zhou, Y.X. Zheng, L.Y. Chen, Negative refraction at the pure Ag/air interface observed in the visible Drude region. *Appl. Phys. Lett.* **93**, 071910 (2008)
4. Y.H. Wu, W. Gu, Y.R. Chen, X.F. Li, X.F. Zhu, P. Zhou, J. Li, Y.X. Zheng, L.Y. Chen, Experimental observation of light refraction going from negative to positive in the visible region at the pure air/Au interface. *Phys. Rev. B* **77**, 035134 (2008)
5. H. Shin, S. Fan, All-angle negative refraction for surface plasmon waves using a metal–dielectric–metal structure. *Phys. Rev. Lett.* **96**, 073907 (2006)
6. E. Verhagen, R. Waele, L. Kuipers, A. Polman, Three-dimensional negative index of refraction at optical frequencies by coupling plasmonic waveguides. *Phys. Rev. Lett.* **105**, 223901 (2010)
7. T. Xu, A. Agrawal, M. Abashin, K.J. Chau, H.J. Lezec, All-angle negative refraction and active flat lensing of ultraviolet light. *Nature* **497**, 470–474 (2013)
8. M. Laue, Die, Warmestrahlung in absorbierenden Körpern. *Ann. Phys.* **32**, 1085–1094 (1910)
9. J.A. Stratton, *Electromagnetic theory* (McGraw-Hill Book Company Inc, New York, 1941)
10. Adler RB, Chu LJ, Fano RM, *Electromagnetic energy transmission and radiation* Ch. 7 and 8, (Wiley, New York, 1960)
11. M.A. Dupertuis, M. Proctor, B. Acklin, Generalization of complex Snell–Descartes and Fresnel laws. *J. Opt. Soc. Am. A* **11**, 1159–1166 (1994)
12. Born, E. Wolf, *Principles of Optics*, 6th ed. (Pergamon, Oxford, 1993), Chap. 13
13. J.L. Garcia-Pomar, M. Nieto-Vesperinas, Transmission study of prisms and slabs of lossy negative index media. *Opt. Express* **12**, 2081–2095 (2004)
14. R.C. Hansen, Negative refraction without negative index. *IEEE Trans. Antennas Propag.* **56**, 402–404 (2008)
15. Z.M. Zhang, B.J. Lee, Lateral shift in photon tunneling studied by the energy streamline method. *Opt. Express* **14**, 9963–9970 (2006)
16. J.W. Chen, H.X. Lu, Generalized laws of reflection and refraction derived from real valued boundary conditions. *Opt. Commun.* **284**, 3802–3807 (2011)
17. N. Sun, Y.M. Mao, J.W. Chen, Y. Zang, W. Wang, Z.K. Tao, G.Z. Xie, Effects of non-synchronized variations of electric and magnetic properties on transmitted waves at lossy interface. *J. Quant. Spectrosc. Radiat. Trans.* **138**, 50–59 (2014)
18. Y. Zang, J.W. Chen, S.Y. He, Theoretical study of visible light refraction phenomena occurring at noble metal–air interfaces. *Opt. Mater.* **46**, 276–281 (2015)
19. W.Q. Chen, M.D. Thoreson, S. Ishii, A.V. Kildishev, V.M. Shalaev, Ultra-thin ultra-smooth and low-loss silver films on a germanium wetting layer. *Opt. Express* **18**, 5124–5134 (2010)
20. EI-Raheem MMA and AI-Baradi AM, Optical properties of as-deposited TiO₂ thin films prepared by DC sputtering technique. *Int. J. Phys. Sci.* **8**, 1570–1580 (2013)
21. R.Q. Wang, J.W. Chen, Theoretical predictions and experimental suggestions for refraction behaviors occurring at lossy interfaces. *J. Opt. Soc. Am. B* **32**, 1955–1960 (2015)